Proc. Natl. Acad. Sci., India, Sect. A Phys. Sci. (January–March 2017) 87(1):57–72
DOI 10.1007/s40010-016-0283-z

RESEARCH ARTICLE

Circumferential Waves in Transradially Isotropic Thermoelastic Spherical Curved Plates

N. Sharma[1]

Received: 6 January 2014 / Revised: 2 June 2016 / Accepted: 4 July 2016 / Published online: 27 July 2016

Abstract This paper presents the propagation of thermoelastic waves along circumferential direction in homogeneous, transradially isotropic spherical curved plates. Mathematical modeling of the problem to obtain dispersion curves for transversely isotropic thermally conducting spherically curved elastic plates leads to coupled differential equations. The coupled differential equations of motion and heat conductions equation in conjunction with stress free, rigidly fixed thermal boundary conditions on the inner and outer surfaces of a spherical curved plate are solved with matrix Fröbenius method. In order to illustrate theoretical development, numerical solutions are obtained and presented graphically for a zinc, cobalt and silicon nitride plate. The graphical results are compared with the available literature. Thermal variations for the non-axially symmetric case of plane strain vibrations, these modes remain coupled and are affected by temperature change. Moreover, these vibration modes are found to be dispersive in nature.

Keywords Spherical curved plates · Matrix Frobenius method · Lowest frequency · Damping factor

✉ N. Sharma
niveditanithmr@gmail.com

[1] Department of Mathematics, National Institute of Technology, Hamirpur 177005, India

1 Introduction

The phenomenon of thermoelastic material finds a wide range of applications in all fields of science including atomic physics, industrial engineering, thermal power plants, submarine structures, pressure vessel, aerospace, chemical pipes and metallurgy. The spherically curved plate, like structures are used in pressure vessels, spherical domes of power plants in addition to many other industrial applications. For non-destructive evaluation of such spherical structures, the mechanics of elastic wave propagation in spherical curved plates must be understood. The current literature shows some valuable studies on Rayleigh surface wave propagation in isotropic solids with spherical boundaries.

The phenomenon of elastic wave propagation in cylindrical structures has received a significant attention recently [1–5]. Shah et al. [6] have analyzed three-dimensional hollow spheres using shell theory and found that the characteristic frequency equation is independent of the longitudinal wave number. Buldyev and Lanin [7] studied the surface wave propagation in solids with curved boundary conditions. Wang et al. [8] studied the stress wave- propagation in orthotropic laminated spherical shells subjected to arbitrary radial dynamic load with the help of finite Hankel transforms and Laplace transforms. Towfighi et al. [9, 10] studied the guided wave propagation problem in circumferential direction of cylindrical curved plate. Towfighi and Kundu [11] studied wave propagation of anisotropic spherical curved plates. Sharma and Pathania [12] investigated the generalized wave propagation in circumferential direction of transversely isotropic cylindrical curved plates. Yu et al. [13] used an orthogonal polynomial series expansion approach for determining the guided wave dispersion curves and

the distribution of displacements in homogeneous anisotropic spherical curved plates based on three-dimensional elasticity and compared the results with Towfighi and Kundu [11]. Yu et al. [14] used a Legendre orthogonal polynomial series expansion approach for determining the characteristics of guided waves in continuous functionally graded piezoelectric materials as spherical curved plates. They reported the influence of radius to thickness ratio on dispersion curves. Yu et al. [15] presented an elastodynamic solution for the stress wave propagation in spherical curved plates composed of functionally graded materials. Yu and Xue [16] investigated the propagation of thermoelastic waves in orthotropic spherical curved plates subjected to stress-free, isothermal boundary conditions in context of the Green-Naghdi (GN) generalized thermoelastic theory. Yu and Dong [17] solved linearized three-dimensional piezoelasticity equations through orthogonal polynomial approach and determined the elastic wave propagation modes in a piezoelectric spherical curved plate. Sharma et al. [18] focused on the analysis of free vibrations of axisymmetric functionally graded hollow spheres. The material is assumed to be graded in radial direction with a simple power law.

The spherically curved plate like structures are used in pressure vessels, spherical domes of power plants in addition to many other industrial applications. From the perspective of non-destructive evaluation of such spherical structures, it is important to understand the mechanics of elastic wave propagation in spherical curved plates through various mathematical techniques. The current literature shows some valuable studies on Rayleigh surface wave propagation in isotropic solids with spherical boundaries. Considering various applications of spherical curved plates in industrial applications, it is proposed to model and study the propagation of circumferential waves in transradially isotropic and thermally conducting spherically curved elastic plates. The partial differential equations of motion and heat conduction along with boundary conditions on the inner and outer surfaces of a spherical curved plate constitute the mathematical model for this problem. The model has been solved using matrix Fröbenius method. The numerical solutions have also been obtained and presented for zinc, cobalt and silicon nitride material plate. It is expected that the wave characteristics may remain coupled and may be affected by temperature changes except for purely shear-harmonic (SH) wave motion wherein they get decoupled and have no effect of temperature. The obtained results compared with those existing in literature to validate the present approach and brief summary of the present work is given at the end of the paper.

2 Formulation and Solution

We consider a homogeneous, transversely isotropic, thermally conducting, elastic spherical curved plate with inner and outer radii a and b respectively. The plate is assumed initially at uniform temperature T_0 in the undisturbed state. The geometry of the problem is shown in Fig. 1 and we considered the problem of wave propagation in the direction of the curvature. Here we represent wave carrier by different names like a curved plate/a spherical plate/a pipe segment or simply a pipe (all these nouns represent wave carrier only). Moreover, we do not include the reflected guided waves from the plate boundary. The considered geometry of the problem can be a segment of a sphere or a complete sphere. But we focus on analysis of the dispersive waves in the curved plate for waves propagating from section S_1 to S_2 (see Fig. 1). Clearly, the wave speed is proportional to radius of curvature. According to Towfighi and Kundu [11] the wavefront on the surface of a spherical shell is assumed to be toroidal. To study wave propagation in a spherical plate segment, the points S_1 and S_2 is aligned along the equator of a sphere by adjusting the positions of north and south poles. Therefore, in order to study the wave propagation between two points in a spherical plate segment, it is sufficient to solve the governing equations for $\theta = \frac{\pi}{2}$ only. The linear governing equations of motion and heat conduction in the absence of body forces and heat sources for a thermoelastic spherical structure have been considered here. These govern the displacement $\vec{u} = (u_r, u_\theta, u_\phi)$ and temperature change $T(r, \phi, t)$ in the plate and are given by Dhaliwal and Singh [19]:

$$\sigma_{rr,r} + \frac{1}{r}\sigma_{r\phi,\phi} + \frac{1}{r}\left[2\sigma_{rr} - \sigma_{\theta\theta} - \sigma_{\phi\phi}\right] = \rho\ddot{u}_r \tag{1}$$

$$\sigma_{r\phi,r} + \frac{1}{r}\sigma_{\phi\phi,\phi} + \frac{3}{r}\sigma_{r\phi} = \rho\ddot{u}_\phi \tag{2}$$

$$\sigma_{r\theta,r} + \frac{1}{r}\sigma_{\phi\theta,\phi} + + \frac{3}{r}\sigma_{r\theta} = \rho\ddot{u}_\theta \tag{3}$$

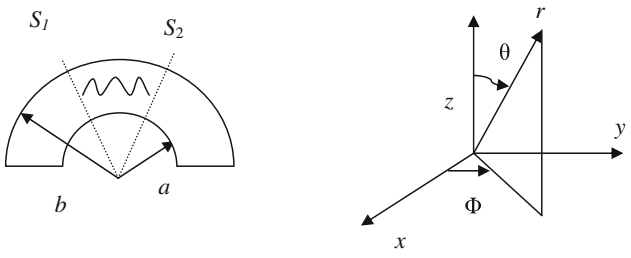

Fig. 1 Geometry of the problem

$$K_3\left(T_{rr}+\frac{2}{r}T_{,r}\right)+K_1\frac{1}{r^2}T_{,\phi\phi}\ -\rho C_e\dot{T} = T_0\left[\beta_1\left(\dot{e}_{\theta\theta}+\dot{e}_{\phi\phi}\right)+\beta_3\dot{e}_{rr}\right] \tag{4}$$

where

$$\sigma_{\theta\theta}=c_{11}e_{\theta\theta}+c_{12}e_{\phi\phi}+c_{13}e_{rr}-\beta_1 T,\quad \sigma_{r\theta}=2c_{44}e_{r\theta}$$
$$\sigma_{\phi\phi}=c_{12}e_{\theta\theta}+c_{11}e_{\phi\phi}+c_{13}e_{rr}-\beta_1 T,\quad \sigma_{r\phi}=2c_{44}e_{r\phi} \tag{5}$$

$$\sigma_{rr}=c_{13}e_{\theta\theta}+c_{13}e_{\phi\phi}+c_{33}e_{rr}-\beta_3 T,\quad \sigma_{\theta\phi}=2c_{66}e_{\theta\phi}$$
$$e_{rr}=\frac{\partial u_r}{\partial r},\quad e_{\theta\theta}=\frac{u_r}{r},\quad e_{\phi\phi}=\frac{1}{r}\frac{\partial u_\phi}{\partial\phi}+\frac{u_r}{r}$$
$$e_{r\phi}=\frac{1}{2}\left[\frac{1}{r}\frac{\partial u_r}{\partial\phi}-\frac{u_\phi}{r}+\frac{\partial u_\phi}{\partial r}\right],\quad e_{r\theta}=\frac{1}{2}\left[\frac{\partial u_\theta}{\partial r}-\frac{u_\theta}{r}\right]$$
$$e_{\phi\theta}=\frac{1}{2}\left[\frac{\partial u_\theta}{\partial\phi}\right]. \tag{6}$$

Here c_{11}, c_{12}, c_{13}, c_{33} and c_{44} are isothermal elastic parameters; α_1, α_3 are the coefficient of Linear thermal expansion, K_1, K_3 are the coefficients of thermal conductivities, along and perpendicular to the axis of symmetry, ρ and C_e, are the density and specific heat at constant strain respectively. The comma notation is used for spatial derivatives and the superposed dot denotes time differentiation. Sharma and Sharma [20] proved thermodynamically that $K_1>0$, $K_3>0$ and of course $\rho>0$ and $T_0>0$. In addition it is proved that $C_e>0$ and the isothermal elasticities are components of a positive definite fourth-order tensor. The necessary and sufficient conditions for the satisfaction of latter requirements are

$$c_{11}>0,\ c_{11}>c_{12},\ c_{11}^2>c_{12}^2,\ c_{44}>0, c_{33}(c_{11}+c_{12})>c_{13}^2. \tag{7}$$

On substituting Eqs. (5) and (6) by Eqs. (1)–(4) the governing differential equations in non-dimensional form are obtained and are given as:

$$u_{\theta,rr}-\frac{2}{r}u_{\theta,r}+\frac{1}{r^2}u_\theta+\frac{(c_1-c_2)}{2r^2}u_{\theta,\phi\phi}+\frac{3}{r}\left(u_{\theta,r}-\frac{u_\theta}{r}\right)-\ddot{u}_\theta=0 \tag{8}$$

$$c_4u_{r,rr}+\frac{2c_4}{r}u_{r,r}+\frac{2(c_3-c_1-c_2)}{r^2}u_r+\frac{1}{r^2}u_{r,\phi\phi}+\frac{1+c_3}{r}u_{\phi,r\phi}+\frac{c_3-c_1-c_2-1}{r^2}u_{\phi,\phi}-\ddot{u}_r-\beta*\left(\frac{\partial}{\partial r}+\frac{2}{r}-\frac{2\bar{\beta}}{r}\right)T=0 \tag{9.1}$$

$$u_{\phi,rr}+\frac{2}{r}u_{\phi,r}-\frac{2}{r^2}u_\phi+\frac{c_1}{r^2}u_{\phi,\phi\phi}+\frac{(1+c_3)}{r}u_{r,r\phi}+\frac{2+c_1+c_2}{r^2}u_{r,\phi}-\ddot{u}_\phi-\frac{\bar{\beta}\beta*T_{,\phi}}{r}=0 \tag{9.2}$$

$$T_{,rr}+\frac{2}{r}T_{,r}+\frac{1}{r^2}T_{,\phi\phi}-\Omega^*\dot{T}-\varepsilon^*\Omega^*\left(\dot{u}_{r,r}+\left(\frac{2}{r}\dot{u}_r+\frac{1}{r}\dot{u}_{\phi,\phi}\right)\bar{\beta}\right)=0 \tag{9.3}$$

We define:

$$\left.\begin{aligned}&\zeta=r/R,\ U_i=u_i/R,\ \tau_{ij}=\frac{\sigma_{ij}}{c_{44}},\ \varepsilon_T=\frac{\beta_3^2T_0}{\rho C_e c_{44}},\ \varsigma_1=a/R,\\&\varsigma_2=b/R,\ c_1=\frac{c_{11}}{c_{44}},c_2=\frac{c_{12}}{c_{44}},\ c_3=\frac{c_{13}}{c_{44}},\ c_4=\frac{c_{33}}{c_{44}},\ \varepsilon^*=\frac{\varepsilon_T\Omega^*}{\beta^*},\\&\bar{\beta}=\frac{\beta_1}{\beta_3},\ \bar{K}=\frac{K_1}{K_3},\ \tau=\frac{v_s}{R}t,\ T'=\frac{T}{T_0},\ \Omega^*=\frac{\omega^*R}{v_s},\beta^*=\frac{\beta_1T_0}{c_{44}}\end{aligned}\right\} \tag{10}$$

Here dashes are ignored for convenience, $\omega^{\cdot}=\frac{C_ec_{44}}{K_3}$ is the thermoelastic characteristic frequency of the plate and $v_s^2=\frac{c_{44}}{\rho}$ shear wave velocity in the medium respectively and the quantity ε is called the thermoelastic coupling parameters.

Introducing quantities (10) in Eqs. (8) and (9), we obtain

$$\left(\frac{\partial^2}{\partial\zeta^2}+\frac{2}{\zeta}\frac{\partial}{\partial\zeta}+\frac{1}{\zeta^2}-\frac{\partial^2}{\partial\tau^2}\right)U_\theta+\frac{(c_1-c_2)}{2\zeta^2}\frac{\partial^2}{\partial\phi^2}U_\theta+\frac{3}{\zeta}\left(\frac{\partial}{\partial\zeta}-\frac{1}{\zeta}\right)U_\theta=0 \tag{11}$$

$$\left(c_4\left(\frac{\partial^2}{\partial\zeta^2}+\frac{2}{\zeta}\frac{\partial}{\partial\zeta}\right)+\frac{2(c_3-c_1-c_2)}{\zeta^2}-\frac{\partial^2}{\partial\tau^2}\right)U_\zeta+\frac{1}{\zeta^2}\frac{\partial^2}{\partial\phi^2}U_\zeta+\frac{1+c_3}{\zeta}\frac{\partial^2}{\partial\zeta\partial\phi}U_\phi+\frac{c_3-c_1-c_2-1}{\zeta^2}\frac{\partial}{\partial\phi}U_\phi-\beta^*\left(\frac{\partial}{\partial\zeta}+\frac{2}{\zeta}-\frac{2\bar{\beta}}{\zeta}\right)\Theta=0 \tag{12}$$

$$\left(\frac{\partial^2}{\partial\zeta^2}+\frac{2}{\zeta}\frac{\partial}{\partial\zeta}+\frac{1}{\zeta^2}-\frac{\partial^2}{\partial\tau^2}\right)U_\phi+\frac{c_1}{\zeta^2}\frac{\partial^2}{\partial\phi^2}U_\phi+\frac{(1+c_3)}{\zeta}\frac{\partial}{\partial\zeta\partial\phi}U_\zeta+\frac{2+c_1+c_2}{\zeta^2}\frac{\partial}{\partial\phi}U_\zeta-\frac{\bar{\beta}\beta*}{\zeta}\frac{\partial\Theta}{\partial\phi}=0 \tag{13}$$

$$\left(\frac{\partial^2}{\partial\zeta^2}+\frac{2}{\zeta}\frac{\partial}{\partial\zeta}+\frac{1}{\zeta^2}-\Omega^*\frac{\partial}{\partial\tau}\right)\Theta-\varepsilon^*\Omega^*\frac{\partial}{\partial\tau}\left(U_{\zeta,\zeta}+\left(\frac{2}{\zeta}\frac{\partial U_\zeta}{\partial\zeta}+\frac{1}{\zeta}\frac{\partial U_\phi}{\partial\phi}\right)\bar{\beta}\right)=0 \tag{14}$$

For further simplification of the Eqs. (11)–(14), we introduce the following transformations

$$\left.\begin{aligned}U_\zeta&=\bar{U}/\sqrt{\zeta}\\U_\theta&=\bar{V}/\sqrt{\zeta}\\U_\phi&=\bar{W}/\sqrt{\zeta}\\\Theta&=\bar{\Theta}/\sqrt{\zeta}\end{aligned}\right\} \tag{15}$$

In light of the transformation (15), the Eqs. (11)–(14), upon simplification provide us

$$\left(\frac{\partial^2}{\partial\zeta^2}+\frac{1}{\zeta}\frac{\partial}{\partial\zeta}-\frac{9}{4\zeta^2}+\frac{c_1-c_2}{\zeta^2}+\frac{c_1-c_2}{2\zeta^2}\frac{\partial^2}{\partial\phi^2}-\frac{\partial^2}{\partial\tau^2}\right)\bar{V}=0 \tag{16}$$

$$\begin{aligned}&\left[c_4\left(\frac{\partial^2}{\partial\zeta^2}+\frac{1}{\zeta}\frac{\partial}{\partial\zeta}--\frac{1}{4\zeta^2}\right)-\frac{2(c_1-c_3+c_2)}{\zeta^2}+\frac{1}{\zeta^2}\frac{\partial^2}{\partial\phi^2}-\frac{\partial^2}{\partial\tau^2}\right]\bar{W}\\&-\left[\frac{1+c_3}{\zeta}\left(\frac{\partial}{\partial\zeta}-\frac{1}{\zeta}-\frac{1}{2\zeta}\right)+\frac{1}{\zeta^2}(2c_3-c_1-c_2)\right]\frac{\partial^2}{\partial\phi^2}\bar{U}\\&-\beta^*\left(\frac{\partial}{\partial\zeta}-\frac{1}{2\zeta}+\frac{2}{\zeta}-\frac{2\bar{\beta}}{\zeta}\right)\bar{\Theta}=0\end{aligned} \tag{17}$$

where $U(\zeta)$, $V(\zeta)$, $W(\zeta)$ and $\Theta^*(\zeta)$ represent the amplitude of vibration in the radial and two tangential directions, m is the magnitude of wave vector along wave propagation direction, and ς_2 is the non-dimensional outer radius of the plate.

Upon using solution (20) in Eqs. (16)–(19) and further simplifying, we obtain

$$\nabla_2^2+\left(1-\eta_0^2/\xi^2\right)V=0 \tag{21}$$

$$\begin{bmatrix} c_4\nabla_2^2 & im\varsigma_2\left(\frac{1+c_3}{\xi}\frac{\partial}{\partial\zeta}-\mu_1^2/\xi^2\right) & -\Omega^{-1}\beta^*\left(\frac{\partial}{\partial\xi}+\frac{3-4\bar{\beta}}{2\xi}\right)\\ im\varsigma_2\left(\frac{1+c_3}{\xi}\frac{\partial}{\partial\zeta}+\mu_1^2/\xi^2\right) & \nabla_2^2+\left(1-\mu_2^2/\xi^2\right) & -\frac{im\,\varsigma_2\,\Omega^{-1}\bar{\beta}\beta^*}{\xi}\\ i\varepsilon^*\,\Omega^*\left(\frac{\partial}{\partial\xi}+\frac{4\bar{\beta}-1}{2\xi}\right) & \frac{i\varepsilon^*\,\Omega^* m\varsigma_2\bar{\beta}}{\xi} & \nabla_2^2+\left(-i\Omega^{-1}-\mu_4^2/\xi^2\right)\end{bmatrix}\begin{bmatrix}U\\W\\\Theta^*\end{bmatrix}=\begin{bmatrix}0\\0\\0\end{bmatrix} \tag{22}$$

$$\begin{aligned}&\left(\frac{\partial^2}{\partial\zeta^2}+\frac{1}{\zeta}\frac{\partial}{\partial\zeta}-\frac{1}{4\zeta^2}+\frac{c_1}{\zeta^2}\frac{\partial^2}{\partial\phi^2}-\frac{2-c_1+c_2}{\zeta^2}+\frac{\partial^2}{\partial\tau^2}\right)\bar{U}\\&+\left(\frac{1+c_3}{\zeta}\left(\frac{\partial}{\partial\zeta}-\frac{1}{2\zeta}\right)+\frac{2+c_1+c_2}{\zeta^2}\right)\bar{W}-\frac{1}{\zeta}\bar{\beta}\beta^*\bar{\Theta}=0\end{aligned} \tag{18}$$

$$\begin{aligned}&\left(\frac{\partial^2}{\partial\zeta^2}+\frac{1}{\zeta}\frac{\partial}{\partial\zeta}-\frac{1}{4\zeta^2}+\frac{\bar{K}}{\zeta^2}\frac{\partial^2}{\partial\phi^2}-\Omega^*\right)\bar{\Theta}\\&-\Omega^*\varepsilon^*\left[\left(\frac{\partial}{\partial\zeta}-\frac{1}{2\zeta}+\frac{2\bar{\beta}}{\zeta}\right)\bar{W}+\frac{\beta}{\zeta}\frac{\partial^2}{\partial\phi^2}\bar{G}\right]=0\end{aligned} \tag{19}$$

According to Yu et al. [13] in toroidal wave travel path, the wave front position is only a function of ϕ because, all points with the same ϕ and for different values of θ are in phase and hence the motion is independent of θ. In a spherical geometry, waves travel a constant angle (ϕ) rather than a constant linear distance in a given time interval. Therefore the toroidal wave travel path length is defined as the product $m\varsigma_2\phi$ which is dimensionally identical to $\Omega\tau$. Thus, the displacement components and temperature of this toroidal has been written as Yu et al. [13]:

$$\left.\begin{aligned}\bar{U}(\zeta,\phi,\tau)&=U(\zeta)\exp(im\varsigma_2\phi+i\Omega\tau)\\\bar{V}(\zeta,\phi,\tau)&=V(\zeta)\exp(im\varsigma_2\phi+i\Omega\tau)\\\bar{W}(\zeta,\phi,\tau)&=W(\zeta)\exp(im\varsigma_2\phi+i\Omega\tau)\\\bar{\Theta}(\zeta,\phi,\tau)&=\Theta^*(\zeta)\exp(im\varsigma_2\phi+i\Omega\tau)\end{aligned}\right\} \tag{20}$$

where

$$\left.\begin{aligned}&\nabla_2^2=\frac{\partial^2}{\partial\xi^2}+\frac{1}{\xi}\frac{\partial}{\partial\xi},\ \xi=\zeta\,\Omega,\ \ \mu_1^2=\frac{3+2(c_1+c_2)-c_3}{2}\\&\mu_2^2=\frac{9+4c_1m^2\varsigma_2^2}{4},\ \ \mu_3^2=\frac{c_4+8(c_1+c_2-c_3)+4m^2\varsigma_2^2}{4}\\&\mu_4^2=\frac{1+4\bar{K}m^2\varsigma_2^2}{4},\ \ \eta_0^2=\frac{9+2(c_1-c_2)m^2\varsigma_2^2}{4}\end{aligned}\right\} \tag{23}$$

Equation (21) gives purely shear wave, which is not affected by temperature change. The solution of Eq. (21) is given as

$$V=\zeta^{-\frac{1}{2}}\left(M_{11}J_{\eta_0}(\zeta\Omega)+M_{12}Y_{\eta_0}(\zeta\Omega)\right)\exp(im\varsigma_2\phi+i\Omega\tau) \tag{24}$$

where J_η and Y_η are the Bessel function of first and second kind and $\eta_0^2=\left(9-2(c_1-c_2)m^2\varsigma_2^2\right)/4>0$ and M_{11} and M_{12} are arbitrary constants to be determined by boundary conditions.

2.1 Matrix Fröbenius Solution

Equation (22) has been solved with the help of matrix Fröbenius method. Clearly the point $r=0$ (i.e.$\xi=0$) is a regular singular point of Eq. (22) and all the coefficients of this differential equations are finite, single valued and continuous in the interval $\eta_1\le\xi\le\eta_2$, where $\eta_1=\varsigma_1\Omega$ and

$\eta_2 = \varsigma_2\Omega$. The field quantities satisfy all the necessary conditions to have series expansions and hence the Fröbenius power series method is applicable to solve the coupled system of differential equations. Thus, we have taken the solution vector of the type

$$Y_n = \sum_{k=0}^{\infty} Z_k \xi^{s+k} \tag{25}$$

where

$$Y_n = [\, U \quad W \quad \Theta^* \,]' \ , \tag{26}$$

$$Z_k = [\, A_k \quad B_k \quad D_k \,]'. \tag{27}$$

Here s is a constant (real or complex) to be determined and A_k , B_k, D_k are unknown coefficients to be determined. We need solution in the domain $\eta_1 \le \zeta \le \eta_2$, $\zeta_1 > 0$. The solution (25) is valid in some deleted interval $0 < \zeta < R'$, $R' > \eta_2$ (about the origin) where R' is the radius of convergence.

Upon substituting solution (25) along with its derivatives in Eq. (22) and simplifying, we get

$$\sum_{k=0}^{\infty} \left[H_1(\upsilon + k)\xi^{-2} + H_2(\upsilon + k)\xi^{-1} + H \right] \xi^{\upsilon+k} Z_{\mathbf{k}} = 0 \tag{28}$$

where

$$\left.\begin{aligned} H &= diag\left(1,\ 1,\ -im\varsigma_2\Omega^{-1}\bar{\beta}\right) \\ H_1(\upsilon + k) &= \left(H_{iq}(\upsilon + k)\right),\ \ i, q = 1,\ 2,\ 3 \\ H_2(\upsilon + k) &= \left(H_{iq}(\upsilon + k)\right),\ \ i, q = 1,\ 2,\ 3 \end{aligned}\right\} \tag{29}$$

The non-zero elements, H_{iq} and H'_{iq}, of matrices H_1 and H_2 are given as under:

$$\left.\begin{aligned} H_{11}(\upsilon + k) &= \left(c_4(\upsilon + k)^2 - \mu_3^2\right), \\ H_{12}(\upsilon + k) &= m\varsigma_2\left[(1 + c_3)(\upsilon + k) - \mu_1^2\right], \\ H_{21}(\upsilon + k) &= \left[(1 + c_3)(\upsilon + k) + \mu_1^2\right], \\ H_{22}(\upsilon + k) &= \left((\upsilon + k)^2 - \mu_2^2\right), \\ H_{33}(\upsilon + k) &= \left((\upsilon + k)^2 - \mu_4^2\right) \end{aligned}\right\} \tag{30}$$

$$\left.\begin{aligned} H'_{13}(\upsilon + k) &= -\Omega^{-1}\beta^*\left(\upsilon + k + \frac{3 - 4\bar{\beta}}{2}\right), \\ H'_{23}(\upsilon + k) &= -im\varsigma_2\Omega^{-1}\bar{\beta}\beta^*, \\ H'_{31}(\upsilon + k) &= i\Omega^{-1}\varepsilon^*\Omega^*\left(\upsilon + k + \frac{(4\bar{\beta} - 1)}{2}\right), \\ H'_{32} &= -m\varsigma_2\varepsilon^*\Omega^*\Omega^{-1}\bar{\beta} \end{aligned}\right\} \tag{31}$$

Equating the coefficients of lowest powers of ξ (i.e. coefficient of $\xi^{\upsilon-2} = 0$) to zero in Eq. (28), we obtain:

$$H_1(\mathbf{\upsilon})\hat{Z}_{\mathbf{0}} = 0 \tag{32}$$

where

$$\left.\begin{aligned} \hat{Z}_{\mathbf{0}} &= [\, A_0 \quad B_0 \quad C_0 \,]' \\ H_1(\upsilon) &= H_{iq}(\upsilon) \quad i, q = 1,\ 2,\ 3 \end{aligned}\right\} \tag{33}$$

For the existence of non-trivial solution of Eq. (32) one must have $|H_1(\mathbf{\upsilon})| = 0$, This results in the following system of indicial equations

$$\left.\begin{aligned} \upsilon^4 - A^*\upsilon^2 + D^* &= 0 \\ \upsilon^2 - \mu_4^2 &= 0 \end{aligned}\right\} \tag{34}$$

where

$$\left.\begin{aligned} A^* &= \frac{\mu_3^2 + c_4\mu_2^2 - m\varsigma_2(1 + c_3)^2}{c_4} \\ D^* &= \frac{\mu_2^2\mu_3^2 - m^2\varsigma_2^2\mu_1^4}{c_4} \end{aligned}\right\} \tag{35}$$

The roots of indicial Eqs. (34) are given as

$$\left.\begin{aligned} \upsilon_1^2 &= \frac{A^* + \sqrt{A^{*2} - 4D^*}}{2} \\ \upsilon_2^2 &= \frac{A^* - \sqrt{A^{*2} - 4D^*}}{2} \\ \upsilon_3^2 &= \mu_4^2 \end{aligned}\right\} \tag{36}$$

The roots υ_j $(j = 1,\ 2,\ 3,\ 4,\ 5,\ 6)$ of Eq. (36) are related through the relation $\upsilon_4 = -\upsilon_1$, $\upsilon_5 = -\upsilon_2$, $\upsilon_6 = -\upsilon_3$. Out of these υ_3 is real and the roots υ_1 and υ_2 may be, in general, complex. If s is complex, then leading terms in the series solution (28) are of the type:

$$\begin{aligned} \begin{bmatrix} A_0 \\ B_0 \\ D_0 \end{bmatrix} \xi^s &= Z_0\xi^{s_R + s_I} \\ &= Z_0\xi^{s_R}[\cos(s_I \log \xi) + i \sin(s_I \log \xi)] \end{aligned} \tag{37}$$

According to Neuringer [21], in order to obtain two independent real solutions, it is sufficient to use any one of the complex roots in a part and then taking its real and imaginary parts. The treatment of complex case is unlike that of the real root case with the advantage that the differential equation is required to be solved only once in the former case rather than twice in latter one. For the choice of roots of the indicial equations, Eq. (28) leads to following eigen-vectors:

$$\left.\begin{aligned} Z_0(\upsilon_1) = Z_0(\upsilon_4) &= \begin{bmatrix} 1 \\ Q_B(\upsilon_1) \\ 0 \end{bmatrix} V_0, \\ Z_0(\upsilon_2) = Z_0(\upsilon_5) &= \begin{bmatrix} 1 \\ Q_B(\upsilon_2) \\ 0 \end{bmatrix} V_0, \\ Z_0(\upsilon_3) = Z_0(\upsilon_6) &= \begin{bmatrix} 0 \\ 0 \\ 1 \end{bmatrix} V_0 \end{aligned}\right\} \tag{38}$$

where

$$Q_B(\upsilon_j) = -\frac{(1+c_3)\upsilon_j + a_1^2}{\upsilon_j^2 - a_2^2} = -\frac{c_4\upsilon_j^2 - a_3^2}{im\varsigma_2\left[(1+c_3)\upsilon_j - a_1^2\right]}, \quad (j = 1\ ,\ 2,\ 4,\ 5),$$

V_0 is a constant.

Thus we have

$$\begin{aligned} A_0 &= [1 \quad 1 \quad 0]V_0, \\ B_0 &= [Q_B(1) \quad Q_B(2) \quad 0]V_0, \qquad D_0 = [0 \quad 0 \quad 1]V_0 \end{aligned} \tag{39}$$

Again equating to zero the coefficients of next lowest degree term ξ^{s-1}, which corresponds to $k = 1$, in Eq. (28), we get:

$$H_1(\upsilon_j + 1)Z_1 + H_2(\upsilon_j)Z_0 = 0, \quad j = 1,\ 2,\ 3,\ 4,\ 5,\ 6 \tag{40}$$

Clearly $H_1(\upsilon_j + 1)$ is non singular for each υ_j, therefore we have:

$$Z_1 = -H_1(\upsilon_j + 1)^{-1}H_2(\upsilon_j)Z_0 = D_1^* Z_0 \tag{41}$$

where

$$D_1^* = -H_1(\upsilon_j + 1)^{-1}H_2(\upsilon_j) = \begin{bmatrix} 0 & 0 & A_{13} \\ 0 & 0 & A_{23} \\ A_{31} & A_{32} & 0 \end{bmatrix} \tag{42}$$

where A_{32} is defined in Appendix A1.

Now equating the coefficients of powers of ξ^{s+k} equal to zero, we have

$$\begin{aligned} &H_1(s+k+2)Z_{k+2} = -H_2(s+k+1)Z_{k+1} - HZ_k \\ &k = 0,\ 1,\ 2 \end{aligned} \tag{43}$$

where the matrices H_1, H_2 and H are defined in Eq. (29).

The Eq. (43) implies that:

$$Z_{k+2} = -\left(H_1(\upsilon_j + k + 2)\right)^{-1}\left[H_2(\upsilon_j + k + 1)Z_{k+1} + HZ_k\right] \tag{44}$$

Now putting $k = 0,\ 1,\ 2,\ 3\ldots$ successively we get

$$\begin{aligned} Z_2 &= -\left(H_1(\upsilon_j + 2)\right)^{-1}\left[H_2(\upsilon_j + 1)D_1^* + H\right]Z_0 = D_2^* Z_0 \\ Z_3 &= -\left(H_1(\upsilon_j + 3)\right)^{-1}\left[H_2(\upsilon_j + 2)D_2^* + HD_1^*\right]Z_0 = D_3^* Z_0 \\ Z_4 &= -\left(H_1(\upsilon_j + 4)\right)^{-1}\left[H_2(\upsilon_j + 3)D_3^* + HD_2^*\right]Z_0 = D_4^* Z_0 \\ &\vdots \\ Z_{k+2} &= -\left(H_1(\upsilon_j + k + 2)\right)^{-1}\left[H_2(\upsilon_j + k + 1)D_{k+1}^* + HD_k^*\right]Z_0 \\ &= D_{k+2}^* Z_0 \end{aligned}$$

where $D_0^* = I$, $D_{k+2}^* = -\left(H_1(\upsilon_j + k + 2)\right)^{-1}\left[H_2(\upsilon_j + k + 1)D_{k+1}^* + HD_k^*\right]$, $k = 1,\ 2,\ 3\ldots$

It can be shown that the matrix D_{k+2} has similar form as that of $H_1(\upsilon_j + k + 2)$ for even values of k and it is alike $H_2(\upsilon_j + k + 2)$ for odd values of k. Thus, we have:

$$\left.\begin{aligned} Z_{2k+2} &= D_{2k+2}^* Z_0 \\ Z_{2k+1} &= D_{2k+1}^* Z_0 \end{aligned}\right\} \tag{45}$$

where

$$\left.\begin{aligned} D_{2k+2}^* &= -\left(H_1(\upsilon_j + 2k + 2)\right)^{-1}\left[H_2(\upsilon_j + 2k + 1)D_{2k+1}^* + HD_{2k}^*\right], \\ D_{2k+1}^* &= -\left(H_1(\upsilon_j + 2k + 1)\right)^{-1}\left[H_2(\upsilon_j + 2k)D_{2k}^* + HD_{2k-1}^*\right] \end{aligned}\right\} \tag{46}$$

Upon simplification, we get

$$D_{2k+2}^* = \begin{bmatrix} K_{11} & K_{12} & 0 \\ K_{21} & K_{22} & 0 \\ 0 & 0 & K_{33} \end{bmatrix} \tag{47}$$

$$D_{2k+1}^* = \begin{bmatrix} 0 & 0 & K'_{13} \\ 0 & 0 & K'_{23} \\ K'_{31} & K'_{32} & 0 \end{bmatrix} \tag{48}$$

where K_{ij}, K'_{ij} $(i,\ j = 1,\ 2,\ 3)$ given by Eqs. (A.2)–(A.3) as are defined in Appendix.

2.2 Convergence of the Series

According to Cullen [22], in case of a matrix sequence $\{P_k\}$ in $C_{k\times k}$, we have $Lim_{k\to\infty} P_k = P(\{P_k\} \to P)$ if each of k^2 component sequence converges. That is $Lim_{k\to\infty}\left(ent_{ij}(P_k)\right) = p_{ij}$, $i,\ j = 1,\ 2,\ 3,\ldots,k$. Moreover, if the matrix sequence $\{P_k\}$ and $\{Q_k\}$ converge to matrices P and Q, respectively, then the sequence $\{P_k,\ Q_k\} \to PQ$ and $(\alpha P_k + \beta Q_k) \to \alpha P + \beta Q$ for any $\alpha,\ \beta \in C$.

Further from Eqs. (47)–(48), it can be shown that

$$D_{2k+2}^* \approx o\left(k^{-2}\right)D^* \quad \text{and} \quad D_{2k+1}^* \approx o\left(k^{-1}\right)D^{**} \tag{49}$$

where $D^* = \frac{i\varepsilon^*\Omega^*\Omega^{-1}}{c_4}\mathrm{diag}[1 \quad 0 \quad 1]$ and D^{**} is a 3×3 null matrix.

By using above facts, both the matrices $D_{2k+2}^* \to 0$ and $D_{2k+1}^* \to 0$ as $k \to \infty$. This implies that the series (25) are

absolutely and uniformly convergent having infinite radius of convergence. Therefore, the considered series in Eq. (25) is analytic and hence can be differentiated term by term.

Thus the general solution of Eq. (18) has the form

$$\left.\begin{aligned}(U_\zeta, U_\phi, \Theta)(\zeta\ ,\ \phi\ ,\ \tau) &= \zeta^{\frac{-1}{2}}\sum_{j=1}^{6}\sum_{k=0}^{\infty}E_{jk}(A_k(\upsilon_j),\ B_k(\upsilon_j), C_k(\upsilon_j))(\Omega\zeta)^{\upsilon_j+k}\\ &\quad\times\exp(i(m\varsigma_2\phi+\Omega\tau))\\ U_\theta(\zeta\ ,\ \phi\ ,\ \tau) &= \zeta^{\frac{-1}{2}}(M_{11}J_\eta(\Omega\zeta)+M_{22}Y_\eta(\Omega\zeta))\\ &\quad\times\exp(i(m\varsigma_2\phi+\Omega\tau))\end{aligned}\right\} \tag{50}$$

The unknowns M_{11}, M_{22} and $E_{jk}\,(j = 1, 2, 3, 4, 5, 6)$ can be evaluated by using boundary conditions.

The formal solution for displacements and stresses is given by

$$U_\zeta = \zeta^{\frac{-1}{2}}\sum_{k=0}^{\infty}\sum_{j=1}^{6}E_{jk}A_k(\upsilon_j)(\xi)^{\upsilon_j+k}\exp(i(m\varsigma_2\phi+\Omega\tau)) \tag{51}$$

$$U_\theta = \zeta^{-\frac{1}{2}}\left(M_{11}J_\eta(\xi)+M_{12}Y_\eta(\xi)\right)\exp(i(m\varsigma_2\phi+\Omega\tau)) \tag{52}$$

$$U_\phi = \zeta^{\frac{-1}{2}}\sum_{k=0}^{\infty}\sum_{j=1}^{6}E_{jk}B_k(s_j)(\xi)^{s_j+k}\exp(i(m\varsigma_2\phi+\Omega\tau)) \tag{53}$$

$$\begin{aligned}\tau_{\zeta\zeta} &= \zeta^{\frac{-1}{2}}\{\sum_{j=1}^{6}E_{j0}\{(c_{34}+c_4(\upsilon_j+1))A_0(\upsilon_j)+im\varsigma_2c_3B_0(\upsilon_j)\}\xi^{\upsilon_j-1}\\ &\quad+\sum_{k=0}^{\infty}\sum_{j=1}^{6}E_{jk}\begin{Bmatrix}(c_{34}+c_4(\upsilon_j+k+1))A_{k+1}(\upsilon_j)\\ +im\varsigma_2c_3B_{k+1}(\upsilon_j)-\Omega^{-1}\beta^*C_k(\upsilon_j)\end{Bmatrix}(\xi)^{\upsilon_j+k}\}\\ &\quad\times\exp(i(m\varsigma_2\phi+\Omega\tau))\end{aligned} \tag{54}$$

$$\begin{aligned}\tau_{\zeta\theta} &= \zeta^{-\frac{1}{2}}\left(M_{11}\left(J'_\eta(\xi)-\frac{3}{2\xi}J_\eta(\xi)\right)+M_{12}\left(Y'_\eta(\xi)-\frac{3}{2\xi}Y_\eta(\xi)\right)\right)\\ &\quad\times\exp(i(m\varsigma_2\phi+\Omega\tau))\end{aligned} \tag{55}$$

$$\begin{aligned}\tau_{\zeta\phi} &= \zeta^{\frac{-1}{2}}[\sum_{j=1}^{6}E_{j0}\left\{im\varsigma_2A_0+\left(\upsilon_j-\frac{3}{2}\right)B_0\right\}(\xi)^{s-1}\\ &\quad+\sum_{k=0}^{\infty}\sum_{j=1}^{6}E_{jk}\begin{Bmatrix}im\varsigma_2A_{k+1}+\\ \left(\upsilon_j+k-\frac{1}{2}\right)B_{k+1}\end{Bmatrix}(\xi)^{\upsilon_j+k}]\\ &\quad\times\exp(i(m\varsigma_2\phi+\Omega\tau))\end{aligned} \tag{56}$$

$$\begin{aligned}\frac{\partial\Theta}{\partial\zeta} &= \zeta^{\frac{-1}{2}}\left[\sum_{j=1}^{6}E_{j0}\left(\upsilon_j-\frac{1}{2}\right)C_0(\upsilon_j)(\xi)^{\upsilon_j-1}\right.\\ &\quad\left.+\sum_{k=0}^{\infty}\sum_{j=1}^{6}E_{jk}\left((\upsilon_j+k+1)C_{k+1}(\upsilon_j)\right)(\xi)^{\upsilon_j+k}\right]\\ &\quad\times\exp i(m\varsigma_2\phi+\Omega\tau)\end{aligned} \tag{57}$$

Equations (51)–(57) constitute the formal solution of the system of coupled partial differential equations.

3 Boundary Conditions

The following types of boundary conditions are taken on the surfaces $\zeta = \zeta_1$ (inner surface) and $\zeta = \varsigma_2$ (outer surface) of spherical curved plate. The boundary conditions are:

Set I: Stress free and thermally insulated condition

$$\tau_{\zeta\zeta} = 0,\ \ \tau_{\zeta\theta} = 0,\ \ \tau_{\zeta\phi} = 0,\ \ \frac{\partial\Theta}{\partial\zeta} = 0 \tag{58}$$

Set II: Stress free and isothermal condition

$$\tau_{\zeta\zeta} = 0,\ \ \tau_{\zeta\theta} = 0,\ \ \tau_{\zeta\phi} = 0,\ \ \ \Theta = 0 \tag{59}$$

Set III: Rigidly fixed and thermally insulated condition

$$U_\zeta = 0,\ \ \ U_\theta = 0,\ \ \ U_\phi = 0,\ \ \frac{\partial\Theta}{\partial\zeta} = 0 \tag{60}$$

Set IV: Rigidly fixed and isothermal condition

$$U_\zeta = 0,\ \ \ U_\theta = 0,\ \ \ U_\phi = 0,\ \ \ \Theta = 0 \tag{61}$$

4 Dispersion Relations

In this section we derive the secular equations for a spherical curved plate subjected to traction-free thermally insulated/isothermal or rigidly fixed, thermally insulated/isothermal boundary conditions at the surfaces.

4.1 Stress Free Curved Plate

In this subsection we derive the characteristic equations for stress free, thermally insulated and stress free isothermal spherical curved plate.

Set I:

Upon using the boundary condition (58) in the expressions (54)–(57) at the surface $\xi = \eta_1$ and $\xi = \eta_2$ we get the following equations

$$\sum_{j=1}^{6} E_{j0}\{(c_4(\upsilon_j+1)+c_{34})A_0(\upsilon_j)+im\varsigma_2c_3B_0(\upsilon_j)\}(\eta_i)^{\upsilon_j-1} + \sum_{k=0}^{\infty}\sum_{j=1}^{6} E_{jk}\left\{\begin{array}{l}(c_4(\upsilon_j+k+1)+c_{34})A_{k+1}(\upsilon_j)\\ +im\varsigma_2c_3B_{k+1}(\upsilon_j)-\Omega^{-1}C_k(\upsilon_j)\end{array}\right\}(\eta_i)^{\upsilon_j+k}=0 \tag{62}$$

$$M_{11}\left(J'_\eta(\eta_i)-\frac{3}{2\eta_i}J_\eta(\eta_i)\right)+M_{12}\left(Y'_\eta(\eta_i)-\frac{3}{2\eta_i}Y_\eta(\eta_i)\right)=0 \tag{63}$$

$$\sum_{j=1}^{6} E_{j0}im\varsigma_2A_0(\upsilon_j)+\left(\upsilon_j-\frac{3}{2}\right)B_0(\upsilon_j)(\eta_i)^{\upsilon_j-1}+ \sum_{k=0}^{\infty}\sum_{j=1}^{6} E_{jk}im\varsigma_2A_{k+1}(\upsilon_j)+\left(\upsilon_j+k-\frac{1}{2}\right)B_{k+1}(\upsilon_j)(\eta_i)^{\upsilon_j+k}=0 \tag{64}$$

$$\sum_{j=1}^{6} E_{j0}\left(\upsilon_j-\frac{1}{2}\right)C_0(\upsilon_j)(\eta_i)^{s_j-1} + \sum_{k=0}^{\infty}\sum_{j=1}^{6} E_{jk}\left((\upsilon_j+k+1)C_{k+1}(\upsilon_j)\right)(\eta_i)^{\upsilon_j+k}=0 \tag{65}$$

where $i = 1$ for inner surface and $i = 2$ for outer surface of the spherical curved plate.

Equations (62)–(65) is a system of simultaneous linear algebraic equations in eight unknowns M_{11}, M_{12} and E_{jk}, $(j = 1, 2, 3, 4, 5, 6)$. These are uniformly and absolutely convergent series. Thus the above system of equations can be expressed in compact form as given below:

$$\mathbf{G^0X_0}+\mathbf{G^kX_k}=0 \tag{66}$$

where

$$X_0=[E_{10}\quad E_{20}\quad E_{30}\quad E_{40}\quad E_{50}\quad E_{60}\quad M_{11}\quad M_{12}],\qquad \mathbf{G^0}=\left(G^0_{ij}\right)_{8\times8} \tag{67}$$

$$X_k=[E_{1k}\quad E_{2k}\quad E_{3k}\quad E_{4k}\quad E_{5k}\quad E_{6k}\quad M_{11}\quad M_{12}],\qquad \mathbf{G^k}=\left(G^k_{ij}\right)_{8\times8} \tag{68}$$

$$\left.\begin{array}{l} G^0_{11}=((c_4(\upsilon_1+1)+c_{34})A_0(\upsilon_1)+im\varsigma_2c_3B_0(\upsilon_1))(\eta_1)^{\upsilon_1-1}\\ G^0_{51}=\left(im\varsigma_2A_0(\upsilon_1)+\left(\upsilon_1-\frac{1}{2}\right)B_0(\upsilon_1)\right)(\eta_1)^{\upsilon_1-1}\\ G^0_{71}=\left(\upsilon_1-\frac{1}{2}\right)C_0(\eta_1)^{\upsilon_1-1}\end{array}\right\} \tag{69}$$

$$\left.\begin{array}{l} G^0_{37}=\left(\frac{J_{\eta-1}(\eta_1)-J_{\eta+1}(\eta_1)}{\eta_1}-\frac{3}{2\eta_1^2}J_\eta(\eta_1)\right)\\ G^0_{47}=\left(\frac{J_{\eta-1}(\eta_2)-J_{\eta+1}(\eta_2)}{\eta_2}-\frac{3}{2\eta_2^2}J_\eta(\eta_2)\right)\end{array}\right\} \tag{70}$$

$$\left.\begin{array}{l} G^k_{11}=((c_4(\upsilon_1+k+1)+c_{34})A_{k+1}(\upsilon_1)+im\varsigma_2c_3B_{k+1}(\upsilon_1)\\ \qquad -\Omega^{-1}\beta^*C_k(\upsilon_1))(\eta_1)^{\upsilon_1+k}\\ G^k_{51}=\left(im\varsigma_2A_{k+1}(\upsilon_1)+\left(\upsilon_1+k-\frac{1}{2}\right)B_{k+1}(\upsilon_1)\right)(\eta_1)^{\upsilon_1+k}\\ G^k_{71}=(\upsilon_1+k+1/2)C_{k+1}(\eta_1)^{\upsilon_1+k}\\ G^k_{ij}=G^0_{ij},\ i=3,4\ \text{and}\ j=7,8\\ G^k_{ij}=G^0_{ij}=0,\ i=3,4;\ j=1,2,3,4,5,6\ \text{or}\\ \qquad i=1,2,5,6,7,8;\ j=7,8\end{array}\right\} \tag{71}$$

where $\eta_1 = \Omega\varsigma_1$ and $\eta_2 = \Omega\varsigma_2$.

Here the elements G^0_{ij} and $G^k_{ij}(i = 1, 5, 7;\ j = 2, 3, 4, 5, 6)$ in Eq. (66) are obtained from G^0_{ij} and $G^k_{ij}(i = 1, 5, 7)$ in Eqs. (70) and (71) by replacing υ_1 with υ_j, $(j = 2, 3, 4, 5, 6)$, respectively. The elements G^k_{ij}, G^k_{ij}, $3, 4, 5, 6)$ are written from G^0_{ij} and G^k_{ij} $(i = 1, 5, 7;\ j = 1, 2, 3, 4, 5, 6)$ by replacing η_1 with η_2 therein. The elements G^0_{38}, G^0_{48} are obtained from G^0_{37}, G^0_{47} respectively by replacing Bessel functions of first kind with Bessel function of second kind.

Equation (66) holds if and only if each term vanishes separately. This implies that

$$\mathbf{G^0X_0}=0=0\quad \text{for}\ k=0 \tag{72}$$

$$\mathbf{G^kX_k}=0\quad \text{for}\ k>0 \tag{73}$$

Equations (72) and (73) has a non-trivial solution if and only if

$$|\mathbf{G^0}|=0\quad \text{for}\ k=0 \tag{74}$$

$$|\mathbf{G^k}|=0\quad \text{for}\ k>0 \tag{75}$$

After lengthy but straightforward simplifications and reductions, the determinantal Eqs. (74) and (75) lead to the following secular equations

$$|G^0|=0,\ i,\ j=1,\ 2,\ 3,\ 4,\ 5,\ 6\quad \text{for}\ k=0 \tag{76}$$

$$|G^k|=0,\ i,\ j=1,\ 2,\ 3,\ 4,\ 5,\ 6\quad \text{for}\ k>0 \tag{77}$$

$$\left(J_{\eta-1}(\eta_1)-J_{\eta+1}(\eta_1)-\frac{3}{2\eta_1}J_\eta(\eta_1)\right)\times\left(J_{\eta-1}(\eta_2)-J_{\eta+1}(\eta_2)-\frac{3}{2\eta_2}J_\eta(\eta_2)\right)-\left(Y_{\eta-1}(\eta_1)-Y_{\eta+1}(\eta_1)-\frac{3}{2\eta_1}Y_\eta(\eta_1)\right)\times\left(Y_{\eta-1}(\eta_2)-Y_{\eta+1}(\eta_2)-\frac{3}{2\eta_2}Y_\eta(\eta_2)\right) \tag{78}$$

where

$$\left.\begin{aligned} G_{11}^{0} &= ((c_4(\upsilon_1+1)+c_{34})A_0(\upsilon_1)+im\varsigma_2 c_3 B_0(\upsilon_1))(\eta_1)^{\upsilon_1-1} \\ G_{21}^{0} &= \left(im\varsigma_2 A_0(\upsilon_1)+\left(\upsilon_1-\frac{1}{2}\right)B_0(\upsilon_1)\right)(\eta_1)^{\upsilon_1-1} \\ G_{31}^{0} &= \left(\upsilon_1-\frac{1}{2}\right)C_0(\eta_1)^{\upsilon_1-1} \end{aligned}\right\} \tag{79}$$

$$\left.\begin{aligned} G_{11}^{k} &= ((c_4(\upsilon_1+k+1)+c_{34})A_{k+1}(\upsilon_1)+im\varsigma_2 c_3 B_{k+1}(\upsilon_1) \\ &\quad -\Omega^{-1}\beta^{*}C_k(\upsilon_1))(\eta_1)^{\upsilon_1+k} \\ G_{31}^{k} &= \left(im\varsigma_2 A_{k+1}(\upsilon_1)+\left(\upsilon_1+k-\frac{1}{2}\right)B_{k+1}(\upsilon_1)\right)(\eta_1)^{\upsilon_1+k} \\ G_{51}^{k} &= (\upsilon_1+k+1/2)C_{k+1}(\eta_1)^{\upsilon_1+k} \end{aligned}\right\} \tag{80}$$

The elements $G_{ij}^{0}(j=2,3,4,5,6)$ of determinant Eqs. (76) and (77) are obtained by just replacing υ_j, $j=1$ in $G_{ij}^{0}(j=1,3,5)$ with υ_j, $j=2,3,4,5,6$ while $G_{ij}^{0}(i=2,4,6)$ are obtained by replacing η_1 in $G_{ij}^{0}(i=1,3,5)$ with η_2.

Set II:

Employing the boundary conditions (59) at the surface $\xi=\eta_1$ and $\xi=\eta_2$ via expressions (54)–(56), we obtain a system of simultaneous linear algebraic equations in eight unknowns M_{11}, M_{11} and E_{jk}, $(j=1,2,3,4,5,6)$ as Eqs. (62)–(64), along with the equation as given below:

$$\sum_{k=0}^{\infty}\sum_{j=1}^{6}E_{jk}C_k(\upsilon_j)(\eta_i)^{\upsilon_j+k}=0 \tag{81}$$

The system of linear algebraic homogeneous Eqs. (62)–(64) and (81) are written in compact form as:

$$\mathbf{H^k X_k}=0 \tag{82}$$

where $\mathbf{H^k}=\left(H_{ij}^{k}\right)_{8\times 8}$.

The elements $H_{ij}^{k}=G_{ij}^{k}$ are defined in Eqs. (79) and (80) in the form of G_{ij}^{k} except the element H_{51}^{k} which is given by

$$H_{51}^{k}=C_k(\upsilon_1)(\eta_1)^{\upsilon_1+k} \tag{83}$$

Equation (82) will have a non-trivial solution if and only if the determinant of the coefficients $\mathbf{X_k}$ vanishes. This requirement of nontrivial solution leads to a determinantal Eq. (82) along with the following equation:

$$\left|\mathbf{H^k}\right|=0 \tag{84}$$

The elements $H_{ij}^{k}=G_{ij}^{k}$ are defined in Eq. (80) except the change in the value of H_{51}^{k} i.e. given by

$$H_{51}^{k}=C_k(\upsilon_1)(\eta_1)^{\upsilon_1+k}$$

Equation (84) represents the frequency for stress free spherical curved plate.

4.2 Rigidly Fixed Curved Plate

In this subsection we derive the characteristic equations for rigidly fixed, thermally insulated and rigidly fixed, isothermal spherical curved plate.

Set III:

Upon imposing the boundary conditions (60), we obtain a system of algebraic homogeneous equations as under:

$$\sum_{k=0}^{\infty}\sum_{j=1}^{6}E_{jk}A_k(\upsilon_j)(\eta_i)^{\upsilon_j+k}=0 \tag{85}$$

$$\sum_{k=0}^{\infty}\sum_{j=1}^{6}E_{jk}B_k(\upsilon_j)(\eta_i)^{\upsilon_j+k}=0 \tag{86}$$

$$M_{11}J_\eta(\eta_i)+M_{12}Y_\eta(\eta_i)=0 \tag{87}$$

where $i=1$ for inner surface and $i=2$ for outer surface of spherical curved plate.

Equations (85)–(87) and (65) in eight unknowns M_{11}, M_{12} and E_{jk}, $(j=1,2,3,4,5,6)$ after simplification can be expressed as:

$$\mathbf{F^k X_k}=0 \tag{88}$$

where X_k is defined in (68) and $\mathbf{F^k}=\left(F_{ij}^{k}\right)_{8\times 8}$

$$\left.\begin{aligned} F_{11} &= A_k(\upsilon_1)(\eta_1)^{\upsilon_1+k} \\ F_{31} &= B_k(\upsilon_1)(\eta_1)^{\upsilon_1+k} \\ F_{51} &= (\upsilon_1+k+1/2)C_{k+1}(\eta_1)^{\upsilon_1+k} \end{aligned}\right\} \tag{89}$$

$$F_{57}=J_\eta(\eta_1) \tag{90}$$

The elements $F_{lj}(j=2,3,4,5,6)$ of Eq. (89) are obtained by replacing $\upsilon_j, j=1$ in $F_{lj}(l=1,3,5)$ with $\upsilon_j, j=2,3,4,5,6$ while $F_{lj's}(l=2,4,6)$ are obtained by replacing η_1 in $F_{lj}(l=1,3,5)$ with η_2. The element F_{il}, $i=7,8$ and $l=8$ in Eq. (90) are obtained by replacing Bessel's function of first kind J_η with that of second kind Y_η and the elements F_{il} $i=8$ and $l=7,8$ are obtained by replacing η_1 in F_{il} $i=7$ and $l=7,8$ with η_2 respectively

Equation (88) has non-trivial solution if and only if we have

$$\left|\mathbf{F^k}\right|=0 \tag{91}$$

Equation (91) can be split into the following equations:

$$\left|B_{ij}\right|=0,\quad i,\ j=1,2,3,4,5,6 \tag{92}$$

$$\left(J_\eta(\eta_1)Y_\eta(\eta_2)-J_\eta(\eta_2)Y_\eta(\eta_1)\right)=0 \tag{93}$$

$$\left.\begin{aligned} B_{11} &= A_k(\upsilon_1)(\eta_1)^{\upsilon_1+k} \\ B_{31} &= B_k(\upsilon_1)(\eta_1)^{\upsilon_1+k} \\ B_{51} &= (\upsilon_1+k+1/2)C_{k+1}(\eta_1)^{\upsilon_1+k} \end{aligned}\right\} \tag{94}$$

The elements $B_{lj}(j = 2, 3, 4, 5, 6)$ of determinantal Eq. (92) are obtained by replacing $\upsilon_j, j = 1$ in $B_{lj}(l = 1, 3, 5)$ with $\upsilon_j, j = 2, 3, 4, 5, 6$ while $B_{lj's}(l = 2, 4, 6)$ are obtained by replacing η_1 in $B_{lj}(l = 1, 3, 5)$ with η_2.

Set IV:

Invoking the boundary conditions (61) we obtain a homogeneous system of linear algebraic equations in the eight unknowns M_{11}, M_{12} and E_{jk}, $(j = 1, 2, 3, 4, 5, 6)$ given by Eqs. (81) and (85)–(87) above. Upon simplifying this system of equations are expressed in compact form as:

$$\mathbf{F}^{*\mathbf{k}}\mathbf{X}_{\mathbf{k}} = 0 \tag{95}$$

where $\mathbf{F}^{*\mathbf{k}} = \left(F_{ij}^{k}\right)_{8\times 8}$.

The elements F_{ij}^{k} are defined in Eqs. (89) and (90) except the change in value of F_{ij}^{k} given by

$$F_{51}^{k} = C_k(\upsilon_1)(\eta_1)^{\upsilon_1+k} \tag{96}$$

The Eq. (95) has non-trivial solution if and only if we have

$$\left|\mathbf{F}^{*\mathbf{k}}\right| = 0 \tag{97}$$

Equation (97) further split into Eq. (93) along with the following equation

$$\left|F_{ij}^{k}\right| = 0,\ i, j = 1, 2, 3, 4, 6 \tag{98}$$

Equations (92) and (98) represent the frequency equation for spherical curved plate in case of rigidly fixed boundary.

5 Homogeneous Isotropic Curved Plate

The analysis reduces to that of an isotropic spherical plate; we make the choice of material parameters as

$$\begin{aligned} &c_{11} = c_{33} = \lambda + 2\mu,\ c_{12} = c_{13} = \lambda, c_{44} = \mu, \\ &\beta_1 = \beta = \beta_3,\ K_1 = K = K_3. \end{aligned} \tag{99}$$

where λ and μ are the Lame constants. As there is no effect of temperature on SH wave motion. For anisotropic material the Eq. (78) agrees with (14) of Yu et al. [13].

For isotropic materials, Eq. (78) agrees with Eq. (29) of Shah et al. [6]. Equation (78) governs the motion corresponding to the case of shear where only the U_θ displacement occurs. These modes of vibrations are not affected by temperature change. Equation (93) again governs the motion corresponding to the case of toroidal shear in the rigidly fixed plate where only U_θ displacement in circumferential direction occurs. These modes of vibrations are not affected by temperature change.

6 Numerical Results and Discussion

In order to illustrate the analytical development we have proposed to carry out some numerical calculations to compute lowest frequency of zinc, cobalt and silicon nitride materials whose physical data are given in Table 1. Due to the presence of dissipation term in heat conduction Eq. (4), the secular equations are, in general, complex transcendental equations which provide us complex values of the frequency (Ω).

We assume that $\Omega = \Omega_R + iD$, where $\Omega_R = \frac{\Omega_R R}{v_s}$ and $D = \frac{\Omega_I R}{v_s}$ denote the lowest frequency and dissipation factor of the vibrations, respectively. Then each of the secular Eq. (77) or (92) is rewritten as $\Omega = f(\Omega)$, which on separating real and imaginary parts provides us the following system of two real equations:

$$\Omega_R = F(\Omega_R, D), \qquad D = G(\Omega_R, D) \tag{100}$$

Table 1 Physical data for zinc, cobalt and silicon nitride crystals

Quantity	Units	Dhaliwal and Singh [19]		Silicon nitride SiN_4 Yu and Xue [16]
		Zinc	Cobalt	
c_{11}	Nm^{-2}	1.628×10^{11}	3.701×10^{11}	5.74×10^{11}
c_{12}	Nm^{-2}	0.362×10^{11}	1.650×10^{11}	1.27×10^{11}
c_{13}	Nm^{-2}	0.508×10^{11}	1.027×10^{11}	1.27×10^{11}
c_{33}	Nm^{-2}	0.627×10^{11}	3.581×10^{11}	4.33×10^{11}
c_{44}	Nm^{-2}	0.770×10^{11}	1.510×10^{11}	10.8×10^{11}
β_1	$Nm^{-2}\ deg^{-1}$	5.75×10^{6}	7.04×10^{6}	3.22×10^{6}
β_3	$Nm^{-2}\ deg^{-1}$	5.17×10^{6}	6.90×10^{6}	2.71×10^{6}
ρ	$Kg\ m^{-3}$	7.14×10^{3}	8.84×10^{3}	3200
C_e	$J\ K\ g^{-1}\ deg$	3.9×10^{2}	4.27×10^{2}	670

The functions F and G in Eq. (100) are selected in such a way that they satisfy the conditions

$$\left|\frac{\partial F}{\partial \Omega_R}\right| + \left|\frac{\partial F}{\partial D}\right| < 1, \quad \left|\frac{\partial G}{\partial \Omega_R}\right| + \left|\frac{\partial G}{\partial D}\right| < 1 \tag{101}$$

for all Ω_R, D is the neighborhood of the actual root. If $\Omega_0 = (\Omega_{R_0}, D_0)$ be the initial approximation, then we can construct the successive approximations as:

$$\left.\begin{array}{ll} \Omega_{R_1} = F(\Omega_{R_0}, D_0), & D_1 = G(\Omega_{R_1}, D_0) \\ \Omega_{R_2} = F(\Omega_{R_1}, D_1), & D_2 = G(\Omega_{R_2}, D_1) \\ \vdots & \vdots \\ \Omega_{R_j} = F(\Omega_{R_{i-1}}, D_{i-1}), & D_j = G(\Omega_{R_i}, D_{i-1}), \quad i = 0, 1, 2, 3, \ldots \end{array}\right\} \tag{102}$$

The sequence (Ω_{R_n}, D_n) of approximations to the root will converge to the actual root provided the initial guess (Ω_{R_0}, D_0) lies in its neighborhood. For initial value $\Omega_0 = (\Omega_{R_0}, D_0)$, the indicial roots s_j $(j = 1, 2, 3)$ given by Eq. (36) are computed and used along with Eq. (38) in the secular Eqs. (77) and (92) to obtain the current values of Ω_R and D each time which are further used to generate the sequence (44). The process is terminated as and when the condition $|\Omega_{i+1} - \Omega_i| < \varepsilon'$; ε' being arbitrarily small number to be selected at random to achieve the accuracy level, is satisfied. The procedure is continuously repeated for different values of inner radius to thickness ratio of the plate. The numerical computations for lowest frequencies and dissipation factor in plate of zinc, cobalt and silicon nitride materials have been presented in Figs. 2, 3, 4, 5, 6, 7, 8 and 9 for stress free or rigidly fixed boundary conditions. In order to illustrate the analytical developments in the previous sections, we now perform some numerical computations and simulations. The secular Eqs. (77) and (92) contain complete information about the effect of different fields' lowest frequency, ratio of inner

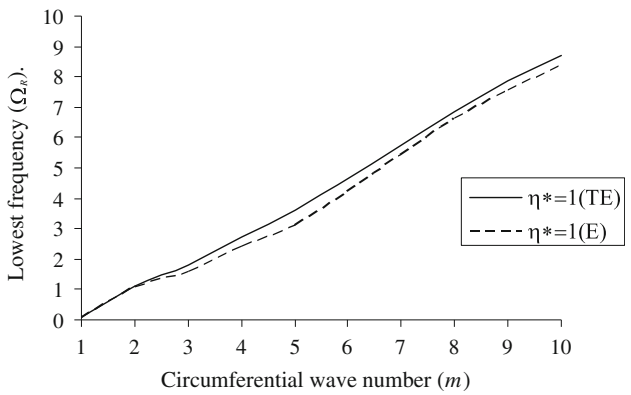

Fig. 2 Variation of lowest frequency with wave number for different values of ratio of inner radius to thickness of the plate for silicon nitride material in stress free case

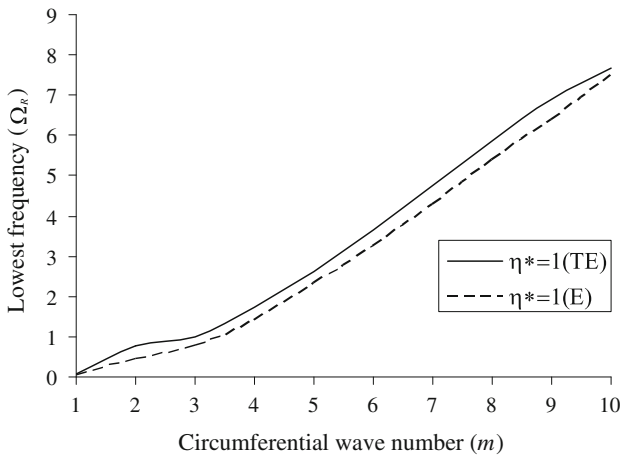

Fig. 3 Variation of lowest frequency with wave number for different values of ratio of inner radius to thickness of the plate for silicon nitride material in rigidly fixed case

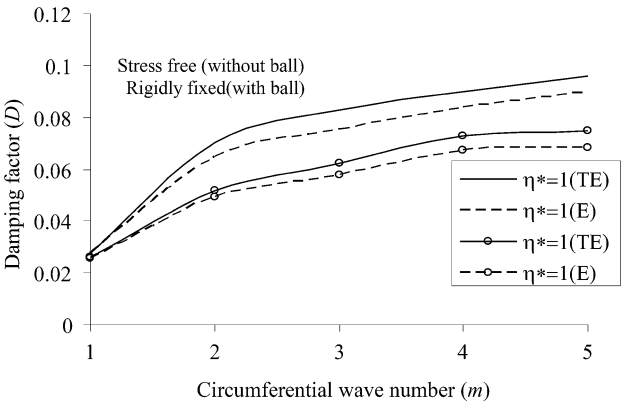

Fig. 4 Variation of damping factor with wave number for different values of ratio of inner radius to thickness of the plate for silicon nitride material

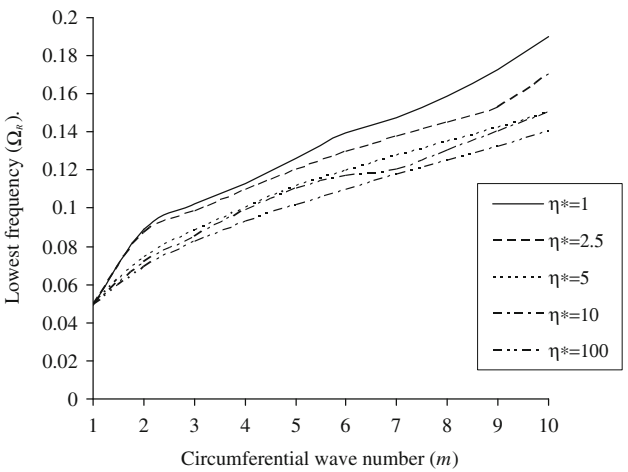

Fig. 5 Variation of lowest frequency with wave number for different values of ratio of inner radius to thickness of the plate for cobalt material

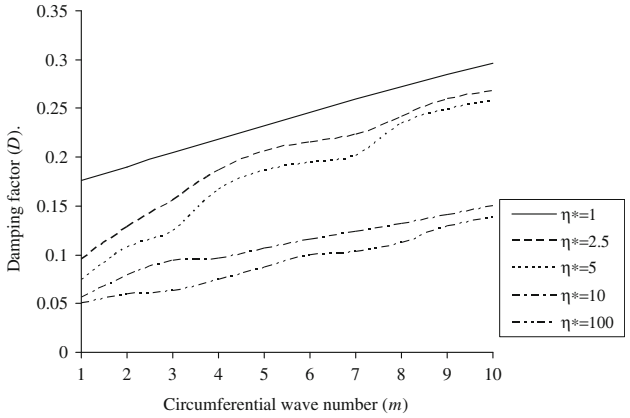

Fig. 6 Variation of damping factor with wave number for different values of ratio of inner radius to thickness of the plate for cobalt material

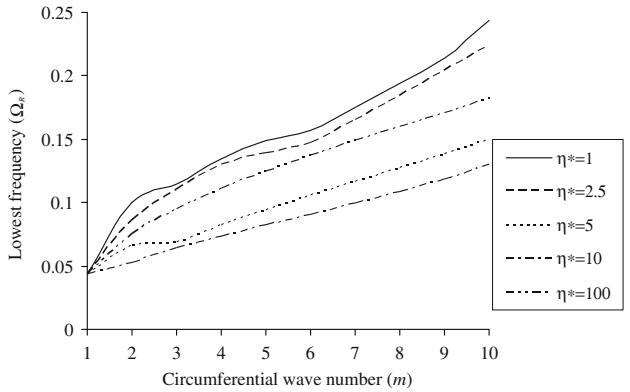

Fig. 7 Variation of lowest frequency with wave number for different values of ratio of inner radius to thickness of the plate for zinc material

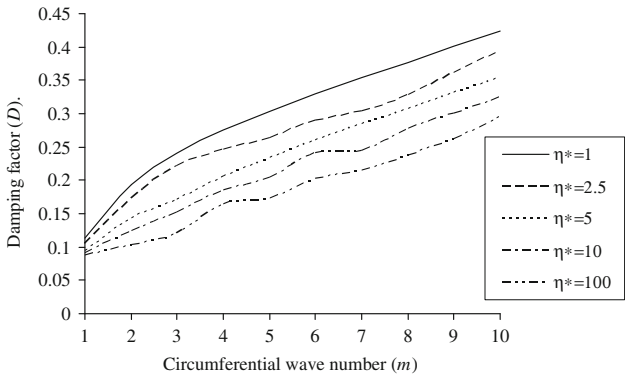

Fig. 8 Variation of damping factor with wave number for different values of ratio of inner radius to thickness of the plate for zinc material

radius to thickness $\eta^* = \frac{\varsigma_1}{\varsigma_2 - \varsigma_1}$ and damping factor (D). The results are presented graphically.

The numerical computations have been performed by employing the iteration technique to the dispersion relation

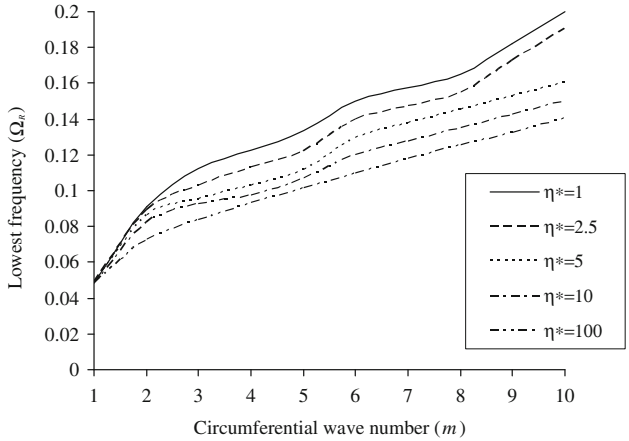

Fig. 9 Variation of lowest frequency with wave number for different values of ratio of inner radius to thickness of the plate for cobalt material rigidly fixed

(77) and (92) with the help of MATLAB programming. The computations have been done for different values of inner radius to thickness ratio (η^*) for fixed outer radius $\zeta_2 = 1.0$.

Figures 2 and 3 show the variations of lowest frequency with respect to the wave number (m) for $\eta^* = 1$ in case of stress free and rigidly fixed boundary conditions for silicon nitride (Si_3N_4) coupled thermoelastic plate and uncoupled (elastic) thermoelastic plates. From the profiles in these figures, it is noticed that the magnitude of lowest frequency increase with wave number (m). The magnitude of vibrations is quite high in thermoelastic (TE) plate as compared to that in elastic (E) plate under considered mechanical conditions, which exhibits the effect of thermal variations.

It is also revealed that the magnitude of lowest frequency increases monotonically for η^* in the absence and presence of thermal field. Moreover, the magnitude of vibrations is large for stress free thermally insulated plate in comparison to rigidly fixed one, depicting the effect of mechanical constraints. These results are similar to the results of Yu and Xue [16] in case of elastic material (in the absence of thermal variations). Figure 4 shows the variations of damping factor with respect to the wave number (m) for $\eta^* = 1$ in case of stress free and rigidly fixed boundary conditions for silicon nitride (Si_3N_4) coupled thermoelastic plate and uncoupled (elastic) thermoelastic plates. It is noticed that damping increases with wave number (m). Also the magnitude of damping is greater for stress free plate in comparison to the rigidly fixed plate.

Figures 5 and 7 show the variation of frequency with wave number for different values of inner radius to thickness ratio (η^*) for zinc and cobalt materials respectively. The dispersion behaviour of Lamb- like waves for circumferential spherical curved plates with different values of inner radius to thickness ratio of the spherical curved

plate is calculated to analyze its influence on dispersion curves. The thickness to mean radius ratio is defined as η^*. From both the figures it is observed that with the increase of wave number the lowest frequency increases in linear fashion. One can see that the influence of η^* on group dispersion curves is obvious. Here frequency increases with the increase of wave number as the η^* decreases the changes are considerably greater for higher value of η^* there is curvilinear increase in frequency while as for lower value of η^* there is almost linear increase in frequency.

Figures 6 and 8 show the variations of dissipation with wave number for different values of η^* for zinc and cobalt materials respectively. The influence of η^* on dissipation is more affected for both materials. For zinc in Fig. 6 for higher value of η^* dissipation increases with the increase of wave number but for lower value of η^* dissipation first increases and then decreases curvilinear for $n > 2$. In case of cobalt material dissipation increases for higher values of η^* and for intermediate value i.e. for $\eta^* = .01$ it shows fluctuating behaviour. It is noticed that there is constant decrease in dissipation for low values of η^*. In microscale SAW devices, the operating frequency is usually very high and the wavelength is very small (i.e. large wave number). It can be seen that the thermal effect is so strong that it influences the dissipation. The effect is significant for higher value of η^*.

Figures 9 and 11 show the variation of frequency with wave number for different values of inner radius to thickness ratio (η^*) for zinc and cobalt materials respectively in case of rigidly fixed boundary conditions. From both the figures it is observed that with the increase of wave number the lowest frequency increases. Figures 10 and 12 show the variations of dissipation with wave number for different values of η^* for zinc and cobalt materials respectively. The influence of η^* on dissipation is more affected for both materials in case of rigidly fixed boundary conditions. It is

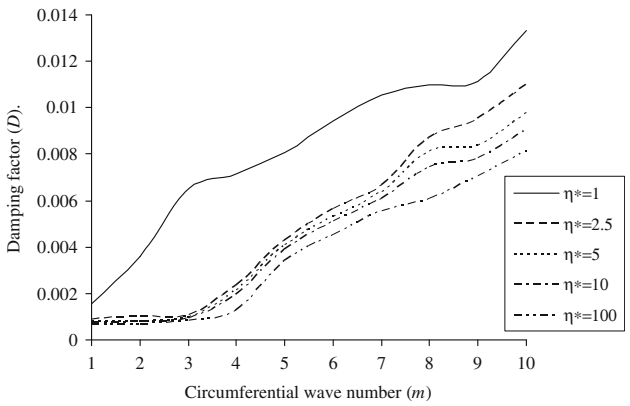

Fig. 10 Variation of damping factor with wave number for different values of ratio of inner radius to thickness of the plate for cobalt material rigidly fixed

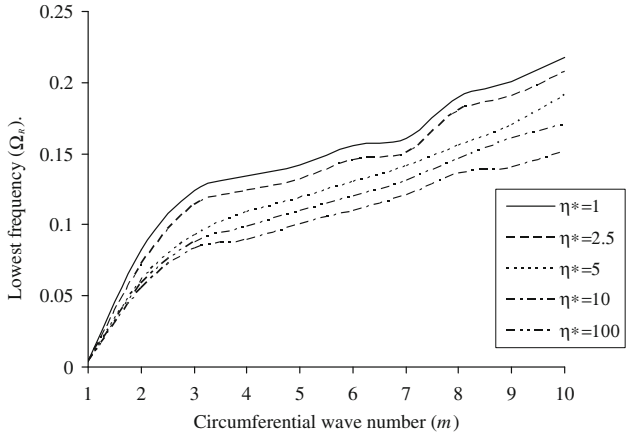

Fig. 11 Variation of lowest frequency with wave number for different values of ratio of inner radius to thickness of the plate for zinc material rigidly fixed

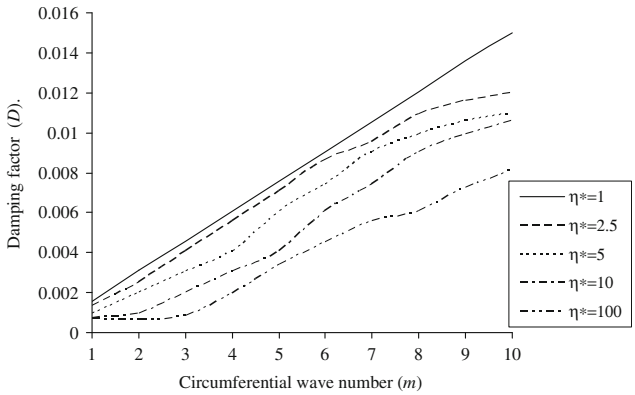

Fig. 12 Variation of damping factor with wave number for different values of ratio of inner radius to thickness of the plate for zinc material rigidly fixed

observed that damping factor increases with increasing value of wave number (m).

Figures 13 and 14 show the variation of non-dimensional phase velocity $\left(v_{ph} = \Omega_R/m\right)$ with circumferential wave number for stress-free and rigidly fixed, thermally insulated boundary for first mode of vibrations for cobalt and zinc materials respectively. From both the figures, it is observed that phase velocities start from large values at vanishing wave number and then exhibit strong dispersion until the velocity flattens out to the value of the thermoelastic Rayleigh wave velocity of the material at higher wave numbers. It is noticed that there is no difference between the plates i.e. spherical curved plate in Fig. 14 with the comparison of cylindrical curved plate given by Sharma and Pathania [6]. Both are made up of zinc material having same outer radius. The dispersion curves are almost similar. The magnitude of phase velocity is noticed to be large for stress free boundary as compared to

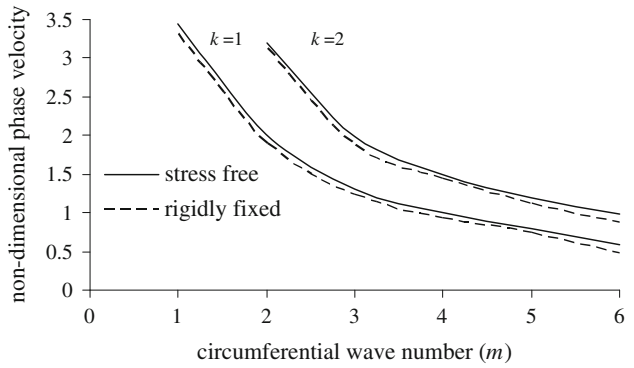

Fig. 13 Variation of non-dimensional phase velocity with wave number for different values k Fröbenius parameter for cobalt material stress free and rigidly fixed boundary conditions

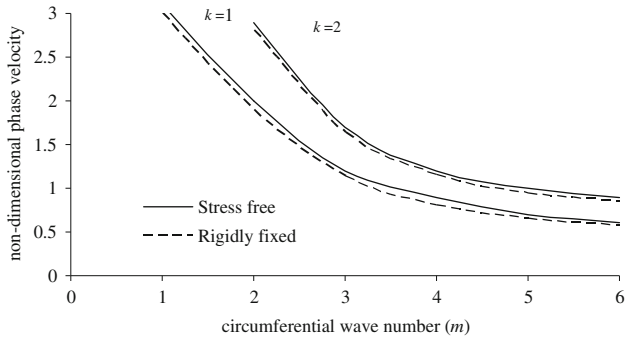

Fig. 14 Variation of non-dimensional phase velocity with wave number for different values k Fröbenius parameter for zinc material stress free and rigidly fixed boundary conditions

that of rigidly fixed boundary conditions depicting the effect of mechanical constraints in the discussed problem.

7 Concluding remarks

After simplifying the system of governing equations of motion and heat conduction equation for a circumferential waves in transradially isotropic spherical curved plate with the help of extended power series method (matrix Frobenius method) is successfully used to obtain exact solution of the resulting system of equations. The concluding remarks are

a. The matrix Fröbenius method has been successfully employed to investigate the vibration characteristics of spherical curved plate structures.
b. It is observed that the shear wave motion of spherical curved plate gets decoupled from the rest of the motion and is not influenced by the thermal field and the corresponding results of pure elastic spherical spherical curved plate are in agreement with those of Shah et al. [6] and Yu et al. [13].
c. It is noticed that the spherical curved plate structures are highly influenced with inner radius to thickness ratio.
d. The lowest frequency has been noticed to increase with the increase of radius to thickness ratio for fixed outer radius.
e. There is small change in damping with the increase of radius to thickness ratio.
f. Almost similar trends of variations of vibration characteristics have been observed for zinc and cobalt material plates under stress free and rigidly fixed boundary conditions.
g. The numerical results for silicon nitride (Si_3N_4) plate compares well with those of Yu and Xue [16] in the absence of thermal variations.
h. It is concluded that the behaviour of phase velocity is similar for cylindrical and spherical curved plates except the change for lower values of wave number. Results for zinc material are in good agreement with earlier results of Sharma and Pathania [12].

Acknowledgments The author is thankful to Late Prof. J. N. Sharma for his encouragement and practical advice for carrying out this part of the work. This work is dedicated to Late Prof. J. N. Sharma who will continue to inspire his students through his teaching and research in the field of mathematics.

Appendix

The quantities $A_{ij}(\upsilon_j),\ i,\ j = 1,\ 2,\ 3$ used in Eq. (42) are defined as below

$$\left.\begin{aligned}
A_{11} &= 0,\\
A_{12} &= 0\\
A_{13} &= \frac{H_{22}(\upsilon_j+1)H'_{13}(\upsilon_j) - H_{12}(\upsilon_j+1)H'_{23}(\upsilon_j)}{H_{11}(\upsilon_j+1)H_{22}(\upsilon_j+1) + H_{12}(\upsilon_j+1)H_{21}(\upsilon_j+1)}\\
A_{21} &= 0,\quad A_{12} = 0\\
A_{23} &= \frac{-H_{21}(\upsilon_j+1)H'_{13}(\upsilon_j) + H_{11}(\upsilon_j+1)H'_{23}(\upsilon_j)}{H_{11}(\upsilon_j+1)H_{22}(\upsilon_j+1) + H_{12}(\upsilon_j+1)H_{21}(\upsilon_j+1)}\\
A_{31} &= \frac{H'_{31}(\upsilon_j)}{H_{33}(\upsilon_j+1)}\\
A_{32} &= \frac{H'_{31}(\upsilon_j)}{H_{33}(\upsilon_j+1)},\\
A_{33} &= 0
\end{aligned}\right\} \tag{103}$$

The quantities $K_{ij}(\upsilon_j),\ K'_{ij}(\upsilon_j)\ \ (i,\ j =\ 1,\ 2,\ 3)$ used in Eqs. (47) and (48) are given by

$$
\left.
\begin{aligned}
K_{11} &= \frac{H_{22}(\upsilon_j+2k+2)}{H^*(\upsilon_j+2k+2)} \\
&\left(H'_{13}(\upsilon_j+2k+1)\frac{H'_{31}(\upsilon_j+2k)}{H_{33}(\upsilon_j+2k+1)}+1\right) \\
&-\frac{H_{12}(\upsilon_j+2k+2)}{H^*(\upsilon_j+2k+2)}H'_{23}(\upsilon_j+2k+2)\left(\frac{H_{21}(\upsilon_j+2k+1)}{H^*(\upsilon_j+2k+1)}H'_{13}(\upsilon_j+2k)+\frac{H_{11}(\upsilon_j+2k+1)}{H^*(\upsilon_j+2k+1)}H'_{23}\right) \\
K_{12} &= \frac{H_{22}(\upsilon_j+2k+2)}{H^*(\upsilon_j+2k+2)}H'_{13}(\upsilon_j+2k+1)\frac{H'_{32}(\upsilon_j+2k)}{H_{22}(\upsilon_j+2k+1)} \\
&-\frac{H_{12}(\upsilon_j+2k+2)}{H^*(\upsilon_j+2k+2)}\left(\frac{H'_{23}(\upsilon_j+2k+1)H'_{32}(\upsilon_j+2k)}{H_{33}(\upsilon_j+2k+1)}-1\right) \\
K_{21} &= \frac{-H_{21}(\upsilon_j+2k+2)}{H^*(\upsilon_j+2k+2)}\left(H'_{13}(\upsilon_j+2k+1)\frac{H'_{31}(\upsilon_j+2k)}{H_{33}(\upsilon_j+2k+1)}+1\right)+\frac{H_{11}(\upsilon_j+2k+2)}{H^*(\upsilon_j+2k+2)} \\
&H'_{23}(\upsilon_j+2k+2)\left(\begin{array}{l}\dfrac{-H_{21}(\upsilon_j+2k+1)}{H^*(\upsilon_j+2k+1)}H'_{23}(\upsilon_j+2k) \\ +\dfrac{H_{11}(\upsilon_j+2k+1)}{H^*(\upsilon_j+2k+1)}H'_{23}(\upsilon_j+2k)\end{array}\right) \\
K_{22} &= \frac{-H_{21}(\upsilon_j+2k+2)}{H^*(\upsilon_j+2k+2)}H'_{13}(\upsilon_j+2k+1)\frac{H'_{32}(\upsilon_j+2k)}{H_{22}(\upsilon_j+2k+1)} \\
&+\frac{H_{11}(\upsilon_j+2k+2)}{H^*(\upsilon_j+2k+2)}\left(\frac{H'_{23}(\upsilon_j+2k+1)H'_{32}(\upsilon_j+2k)}{H_{33}(\upsilon_j+2k+1)}-1\right) \\
K_{33} &= \frac{H'_{31}(\upsilon_j+2k+2)}{H_{33}(\upsilon_j+2k+2)}\left(\begin{array}{l}H_{22}(\upsilon_j+2k+1)\dfrac{H'_{13}(\upsilon_j+2k)}{H^*(s_j+2k+1)}-\dfrac{H_{12}(\upsilon_j+2k+1)H'_{23}(\upsilon_j+2k)}{H^*(s_j+2k+1)} \\ +H'_{32}(\upsilon_j+2k+2)\left(\begin{array}{l}\dfrac{-H_{21}(\upsilon_j+2k+1)H'_{23}(\upsilon_j+2k)}{H^*(\upsilon_j+2k+1)} \\ +\dfrac{H_{11}(\upsilon_j+2k+1)H'_{23}(\upsilon_j+2k)}{H^*(\upsilon_j+2k+1)}\end{array}\right) \\ -i\Omega^*\varepsilon^*\Omega^{-1}\end{array}\right)
\end{aligned}
\right\} \tag{104}
$$

and

$$
\left.
\begin{aligned}
K'_{13} &= \frac{H_{22}(\upsilon_j+2k+1)}{H^*(\upsilon_j+2k+1)}H'_{13}(\upsilon_j+2k) \\
&-\frac{H_{11}(\upsilon_j+2k+2)H'_{23}(\upsilon_j+2k)}{H^*(\upsilon_j+2k+2)} \\
K'_{23} &= \frac{-H_{21}(\upsilon_j+2k+1)H'_{23}(\upsilon_j+2k)}{H^*(\upsilon_j+2k+1)} \\
&+\frac{H_{11}(\upsilon_j+2k+2)H'_{23}(\upsilon_j+2k)}{H^*(\upsilon_j+2k+1)} \\
K'_{31} &= \frac{H'_{31}(\upsilon_j+2k)}{H_{33}(\upsilon_j+2k+1)}, \quad K'_{32} = \frac{H'_{32}(\upsilon_j+2k)}{H_{33}(\upsilon_j+2k+1)}
\end{aligned}
\right\} \tag{105}
$$

References

1. Gazis DC (1959) Three-dimensional investigation of the propagation of waves in hollow circular cylinders. I. Analytical foundation. J Acoust Soc Am 31:568–573
2. Gazis DC (1959) Three-dimensional investigation of the propagation of waves in hollow circular cylinders. II. Numerical results. J Acoust Soc Am 31:573–578
3. Grace OD, Goodman RR (1966) Circumferential waves on solid cylinders. J Acoust Soc America 39:173–174
4. Brekhovskikh LM (1968) Surface waves confined to the curvature of the boundary in solid. Sov Phys-Acoust 13:462–472
5. Armenkas AE, Reitz ES (1973) Propagation of harmonic waves in orthotropic, circular cylindrical shells. ASME J Appl Mech 95:168–174
6. Shah AH, Ramakrishna CV, Datta SK (1969) Three-dimensional and shell theory analysis of elastic waves in a hollow sphere. ASME J Appl Mech 36:431–439

7. Buldyev VS, Lanin AI (1996) Investigation of the interference wave field on the surface of an elastic sphere. In: Collection: numerical methods of solving problems in mathematical physics. Nauka, Moscow, pp 131–143 (in Russian)
8. Wang X, Lu G, Guillow SR (2002) Stress wave propagation in orthotropic laminated thick walled spherical shells. Int J Solids Struct 39(4027):4037
9. Towfighi S (2001) Elastic wave propagation in circumferential direction in anisotropic pipes. PhD dessertation, The University of Arizon, Tucson, AZ-USA
10. Towfighi S, Kundu T, Ehsani M (2002) Elastic wave propagation in circumferential direction in anisotropic cylindrical curved plates. Transactions of the ASME. J Appl Mech 69:283–291
11. Towfighi S, Kundu T (2003) Elastic wave propagation in anisotropic spherical curved plate. Int J Solid Struct 40:5495–5510
12. Sharma JN, Pathania V (2005) Generalized thermoelastic wave propagation in circumferential direction of transversely isotropic cylindrical curved plates. J Sound Vib 281:117–1131
13. Yu JG, Wu B, Huo H, He C (2007) Characteristics of guided waves in anisotropic spherical curved plates. Wave Motion 44:271–281
14. Yu JG, Wu B, Huo H, He C (2007) Wave propagation in functionally graded piezoelectric spherically curved plates. Phys Stat Solut (b) 244:3377–33889
15. Yu JG, Wu B, Hu HL, He CF (2007) Characteristics of guided waves in graded spherical curved plates. Int J Solids Struct 44:3627–3637
16. Yu JG, Xue TL (2010) Generalized thermoelastic waves in spherical curved plates without energy dissipation. Acta Mech 212:39–50
17. Yu JG, Dong SF (2010) Elastic waves in piezoelectric spherical curved plates. Key Eng Mater 455:672–677
18. Sharma DK, Sharma JN, Dhaliwal SS, Walia V (2014) Vibration analysis of axisymmetric functionally graded visco-thermoelastic spheres. Acta Mech Sin 30:100–111
19. Dhaliwal RS, Singh A (1980) Dynamic coupled thermoelasticity. Hindustan Publ Company, New Delhi
20. Sharma JN, Sharma PK (2002) Free vibration analysis of homogeneous transversely isotropic thermoelastic cylindrical panel. J Therm Stress 25:169–182
21. Neuringer JL (1978) The Fröbenius method for complex roots of the indicial equation. Int J Math Educ Sci Technol 9:71–77
22. Cullen CG (1966) Matrices and Linear transformations. Addison-Wesley Publishing Company, Reading